

## Supplementary Materials and Methods

**RNA Synthesis.** A single-stranded DNA oligonucleotide template was purchased from IDT (5' TGCGTTGCGTGTTCGCTGTGTCCATGGTGTATCCTGTCCCTGTTCCATGGCTGTATGGAGGATCTCCAGTATAAGGGATTCTATAGTGTACCTAAATGAATTC 3') containing an SP6 RNA polymerase promoter binding site on the 3' end (underlined) and a reverse transcriptase primer binding site on the 5' end (underlined). The reverse transcription primer binding site (RNA sequence 5' GCGACACGCAACGCA 3') was designed such that it would not interfere with the RNA secondary structure. RNA was synthesized *in vitro* using an SP6 RNA polymerase kit (Ambion). Full length RNA products were isolated with a denaturing 8% PAGE gel and passively eluted overnight in 0.3 M sodium acetate. After ethanol precipitation, the RNA was re-suspended in 0.5 X TE buffer (5 mM Tris, pH = 7.5, 0.5 mM EDTA).

Single-stranded DNA oligonucleotide templates for the mutant RNA sequences were also purchased from IDT: helix 1 destabilizing mutant (5' TGCGTTGCGTGTTCGCTGTGTCCATGGTGTATCCTGCTTTCGTTCCATGGCTGTATGGAGGATCTCCAGTATAAGGGATTCTATAGTGTACCTAAATGAATTC 3'), helix 1 compensatory mutant (5' TGCGTTGCGTGTTCGCTGTGTCCATGGTGTATCCTGCTTTCGTTCCATGGCTGTATGGAGGATCTCCAGTATAGAAAGTTCTATAGTGTACCTAAATGAATTC 3'), helix 2 destabilizing mutant (5' TGCGTTGCGTGTTCGCTGTGTCCATGGTGTATCCTGTTGGTACCCTGTATGGAGGATCTCCAGTATAAGGGATTCTATAGTGTACCTAAATGAATTC 3'), and helix 2 compensatory mutant (5' TGCGTTGCGTGTTCGCTGTGTGGTACCCTGTATCCTGTCCTGTTGGTACCCTGTATGGAGGATCTCCAGTATAAGGGATTCTATAGTGTACCTAAATGAATTC 3'). RNA was synthesized from these using an SP6 RNA polymerase kit (Ambion). After phenol-chloroform extraction and ethanol precipitation, RNA was purified with Illustra Microspinn G-25 Columns (GE Healthcare).

**Chemical Mapping.** For all chemical mapping experiments, 10  $\mu$ L samples with final concentration of 100 mM KCl were prepared as follows: 10 pmol of RNA was combined with buffer (final concentration: 10 mM HEPES for DMS (Sigma-Aldrich) and NMIA (Invitrogen) reactions or 10 mM potassium borate for CMCT (Sigma-Aldrich) with a pH of 7.5 (DMS) or 8.0 (NMIA and CMCT). Samples were annealed at 95  $^{\circ}$ C for 2 min and then placed on ice for 2 min.  $MgCl_2$  was then added to each sample to a final concentration of 10 mM. For samples mapped in the absence of  $Mg^{2+}$ , an equal amount of water was added. Samples were then folded at 37  $^{\circ}$ C for 10 min.

For DMS mapping, 9  $\mu$ L samples were treated with either 1  $\mu$ L of 100% ethanol or 1  $\mu$ L of 1:30, 1:60, or 1:120 dilutions of DMS in 100% ethanol for 5 min. For NMIA mapping, samples were treated with 1  $\mu$ L of DMSO or 1  $\mu$ L of NMIA in DMSO to a final concentration of 12, 6, or 3 mM NMIA for 45 min. CMCT samples were treated with 1  $\mu$ L of water or 1  $\mu$ L of 50, 25, or 12.5 mg/mL CMCT in water for 5 min. All 10  $\mu$ L reactions were carried out at 37  $^{\circ}$ C. After incubation, each sample was ethanol precipitated and re-suspended in 0.5 X TE buffer. Primer extension was carried out as described by Wilkinson et. al.<sup>1</sup> Nucleotide positions were identified using dideoxy sequencing ladders. Primer extension was identical to the experimental samples, but 1  $\mu$ L of A, C, G, or T ddNTP (GE Life Sciences) was added to each reaction.

Samples were run on a denaturing 8% PAGE gel. Gels were exposed to a phosphor screen and images produced via phosphorimager. Chemical mapping reactivities were quantified by densitometry (MyImageAnalysis – Thermo). After subtracting the background, reactivities were normalized against the average of the 10% most reactive nucleotides, excluding outliers. Outliers were defined by being greater than 1.5 times the inter-quartile range, but were capped at 5% of the total number of nucleotides.<sup>2</sup> Any reactivity greater than 0.85 was considered a strong hit. Chemical mapping data are deposited in the public SNRNASM database<sup>3</sup> (<https://docs.google.com/spreadsheets/d/ccc?key=0AinH1hkhQ7eKdG00eEIJJeDhVQVBpMGliLUdIVER2TUE&usp=sharing>).

**Secondary Structure Prediction.** For the native sequence, secondary structure for the condition with  $Mg^{2+}$  was predicted from SHAPE data using ShapeKnots.<sup>4</sup> The program was run using the default parameters and the normalized SHAPE data described above with the following modification. Since the program does not allow negative reactivities, any reactivities between -0.1 and 0 were assigned to be 0 and any reactivities less than -0.1 were omitted. Secondary structure for the condition without  $Mg^{2+}$  was predicted with RNAstructure.<sup>5</sup> The program was run using the default parameters. Any nucleotide classified as a strong hit by DMS, or CMCT was constrained to be single-stranded in the prediction. NMIA data was used as pseudo-energy restraints on the RNAstructure prediction.

For the mutant sequences, secondary structures were predicted using RNAstructure with the same method as the native sequence without  $Mg^{2+}$ . For the two compensatory mutants (Figures 2B and 2D) in the presence of  $Mg^{2+}$ , the chemical mapping data was overlaid on the pseudoknot structure predicted from the native sequence in the presence of  $Mg^{2+}$ .

**Optical Melting.** Melting temperatures of the RNA were determined by optical melting at 260 nm both in the presence and absence of 10 mM  $MgCl_2$ . RNA was prepared as described above but resuspended in 10 mM HEPES, pH=8.0, 100 mM KCl, and 10 mM  $MgCl_2$  (where applicable). The temperature ranged from 25 to 95 °C with a ramp rate of 1 °C/min and measurements were taken every 0.5 °C. MeltWin 3.5<sup>6</sup> was used to subtract the background and plot and analyze the melting curves and their first derivatives.

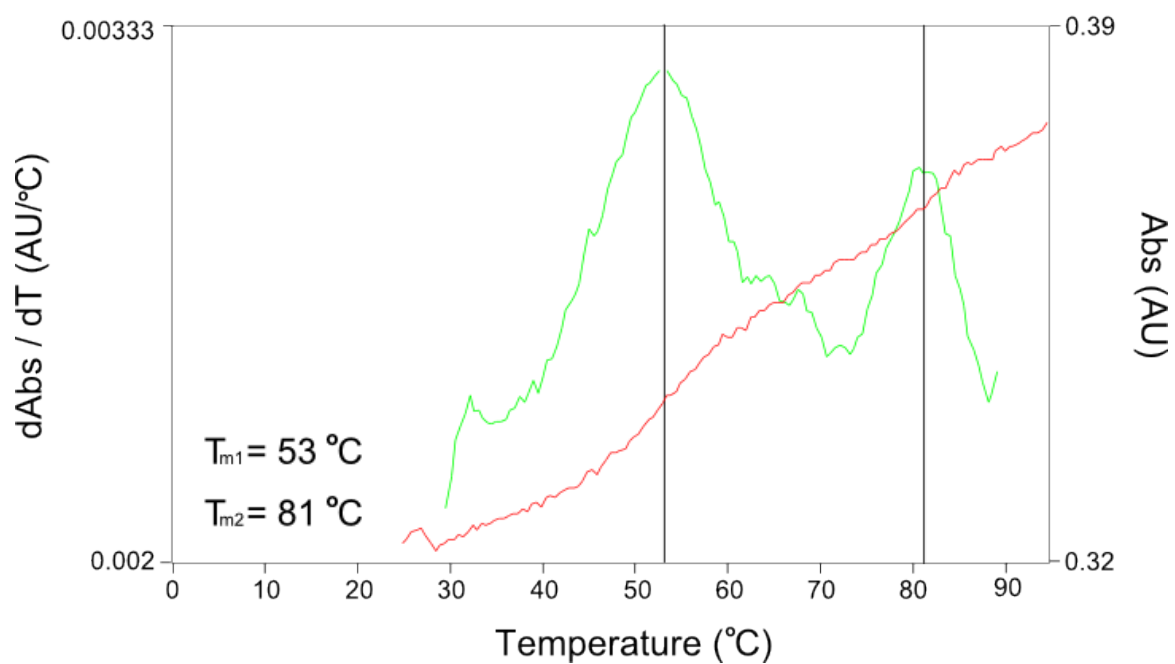
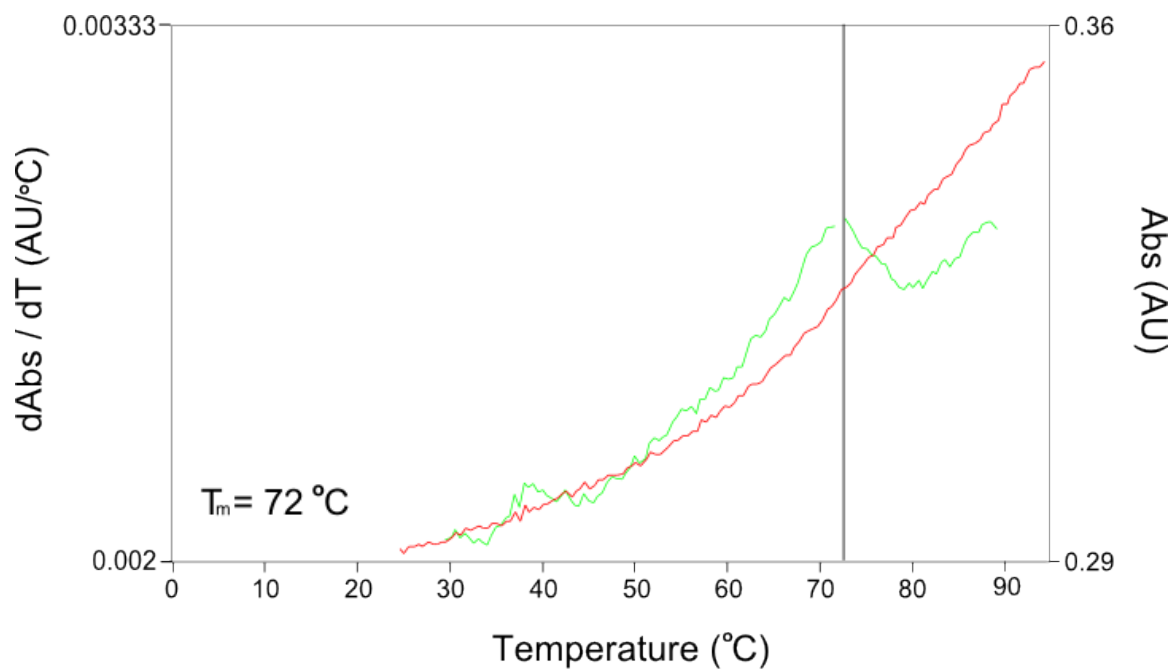


Figure S1: Absorbance (red) and first derivative (green) optical melting curves at 260 nm in the presence (top) and absence (bottom) of 10 mM MgCl<sub>2</sub>.

## References:

1. Wilkinson, K. A., Merino, E. J., and Weeks, K. M. (2006) Selective 2'-hydroxyl acylation analyzed by primer extension (SHAPE): quantitative RNA structure analysis at single nucleotide resolution, *Nat Protoc* *1*, 1610-1616.
2. Deigan, K. E., Li, T. W., Mathews, D. H., and Weeks, K. M. (2009) Accurate SHAPE-directed RNA structure determination, *Proc Natl Acad Sci U S A* *106*, 97-102.
3. Rocca-Serra, P., Bellaousov, S., Birmingham, A., Chen, C., Cordero, P., Das, R., Davis-Neulander, L., Duncan, C. D., Halvorsen, M., Knight, R., Leontis, N. B., Mathews, D. H., Ritz, J., Stombaugh, J., Weeks, K. M., Zirbel, C. L., and Laederach, A. (2011) Sharing and archiving nucleic acid structure mapping data, *RNA* *17*, 1204-1212.
4. Hajdin, C. E., Bellaousov, S., Huggins, W., Leonard, C. W., Mathews, D. H., and Weeks, K. M. (2013) Accurate SHAPE-directed RNA secondary structure modeling, including pseudoknots, *Proc Natl Acad Sci U S A* *110*, 5498-5503.
5. Reuter, J. S., and Mathews, D. H. (2010) RNAstructure: software for RNA secondary structure prediction and analysis, *BMC Bioinformatics* *11*, 129.
6. McDowell, J. A., and Turner, D. H. (1996) Investigation of the structural basis for thermodynamic stabilities of tandem GU mismatches: solution structure of (rGAGGUCUC)<sub>2</sub> by two-dimensional NMR and simulated annealing, *Biochemistry* *35*, 14077-14089.